Am J Physiol Heart Circ Physiol 289: H1209–H1217, 2005.
First published April 29, 2005; doi:10.1152/ajpheart.00046.2005.

Effects of elastin haploinsufficiency on the mechanical behavior of mouse arteries

Jessica E. Wagenseil,[1] Nandan L. Nerurkar,[2] Russell H. Knutsen,[1] Ruth J. Okamoto,[2,3] Dean Y. Li,[4] and Robert P. Mecham[1]

[1]*Department of Cell Biology and Physiology, Washington University School of Medicine, and Departments of* [2]*Biomedical Engineering and* [3]*Mechanical Engineering, Washington University, St. Louis, Missouri; and* [4]*Program in Human Molecular Biology and Genetics, University of Utah, Salt Lake City, Utah*

Submitted 14 January 2005; accepted in final form 26 April 2005

Wagenseil, Jessica E., Nandan L. Nerurkar, Russell H. Knutsen, Ruth J. Okamoto, Dean Y. Li, and Robert P. Mecham. Effects of elastin haploinsufficiency on the mechanical behavior of mouse arteries. *Am J Physiol Heart Circ Physiol* 289: H1209–H1217, 2005. First published April 29, 2005; doi:10.1152/ajpheart.00046.2005.—Supravalvular aortic stenosis (SVAS) is associated with decreased elastin and altered arterial mechanics. Mice with a single deletion in the elastin gene ($ELN^{+/-}$) are models for SVAS. Previous studies have shown that elastin haploinsufficiency in these mice causes hypertension, decreased arterial compliance, and changes in arterial wall structure. Despite these differences, $ELN^{+/-}$ mice have a normal life span, suggesting that the arteries remodel and adapt to the decreased amount of elastin. To test this hypothesis, we performed in vitro mechanical tests on abdominal aorta, ascending aorta, and left common carotid artery from $ELN^{+/-}$ and wild-type (C57BL/6J) mice. We compared the circumferential and longitudinal stress-stretch relationships and residual strains. The circumferential stress-stretch relationship is similar between genotypes and changes <3% with longitudinal stretch at lengths within 10% of the in vivo value. At mean arterial pressure, the circumferential stress in the ascending aorta is higher in $ELN^{+/-}$ than in wild type. Although arterial pressures are higher, the increased number of elastic lamellae in $ELN^{+/-}$ arteries results in similar tension/lamellae compared with wild type. The longitudinal stress-stretch relationship is similar between genotypes for most arteries. Compared with wild type, the in vivo longitudinal stretch is lower in $ELN^{+/-}$ abdominal and carotid arteries and the circumferential residual strain is higher in $ELN^{+/-}$ ascending aorta. The increased circumferential residual strain brings the transmural strain distribution in $ELN^{+/-}$ ascending aorta close to wild-type values. The mechanical behavior of $ELN^{+/-}$ arteries is likely due to the reduced elastin content combined with adaptive remodeling during vascular development.

stress; residual strain; opening angle; compliance; longitudinal

ELASTIN AND COLLAGEN are the principal determinants of passive artery mechanics. Elastin provides reversible extensibility during cyclic loading of the cardiac cycle (22), whereas collagen provides strength and prevents failure at high pressure (11). It is believed that elastin bears load in both the circumferential and longitudinal directions, whereas collagen bears load mostly in the circumferential direction. Elastin is believed responsible for the in vivo longitudinal retraction force in arteries and consequent shortening upon excision. Decreased elastin content with aging, hypertension, and atherosclerosis is accompanied by a decrease in longitudinal retraction force and circumferential compliance (change in diameter for a specified change in pressure) (8). Decreased elastin content also is found in genetic diseases such as supravalvular aortic stenosis (SVAS). SVAS is a congenital narrowing of the large arteries caused by deletions within the elastin gene that lead to functional haploinsufficiency (10). SVAS patients often exhibit hypertension (1) and have thinner and more numerous elastic lamellae (19).

Elastin is encoded by a single gene (ELN); hence, the contribution of elastin to passive artery mechanics can be studied in a controlled manner with genetically modified mice. $ELN^{-/-}$ mice die within a few days of birth as a result of obstructive arterial disease (18). Unfortunately, arteries at this stage are difficult to isolate and manipulate for in vitro tests. $ELN^{+/-}$ mice have a normal life span and, similarly to SVAS patients, exhibit systemic hypertension, thinner and more numerous elastic lamellae, and lower total elastin content. Initial studies of $ELN^{+/-}$ artery mechanics showed decreased compliance in large elastic vessels (10, 19). These measurements, however, were made on ex vivo arterial segments, and no adjustments were made for the effect of longitudinal stretch (25). It is known that arteries are in a stretched state in vivo and that compliance changes with increased stretch. To determine how longitudinal stretch influences compliance and the circumferential stress-stretch relationship, we conducted mechanical testing at different stretch lengths on $ELN^{+/-}$ and wild-type arteries.

Other mechanical properties, such as the longitudinal force-stretch and stress-stretch relationships, in vivo longitudinal stretch, and circumferential residual strain, also may be affected by the decreased amount of elastin in $ELN^{+/-}$ arteries. In vivo longitudinal stretch is defined by the amount an artery retracts upon excision. Circumferential residual strain can be determined from the "opening angle" formed when a ring of arterial tissue is cut radially. Circumferential residual strain serves to normalize the stress and strain distribution through the artery wall (12). To assess the effects of reduced elastin on these mechanical properties, we measured the longitudinal force-stretch and stress-stretch relationships, in vivo longitudinal stretch, and circumferential residual strain in $ELN^{+/-}$ and wild-type arteries.

MATERIALS AND METHODS

Animals. Wild-type C57BL/6J mice ($ELN^{+/+}$) and mice bearing a heterozygous deletion of exon 1 in the elastin gene ($ELN^{+/-}$) (18)

Address for reprint requests and other correspondence: R. P. Mecham, Dept. of Cell Biology and Physiology, CB 8228, Washington Univ. School of Medicine, 660 S. Euclid, St. Louis, MO 63110 (e-mail: bmecham@cellbiology.wustl.edu).

The costs of publication of this article were defrayed in part by the payment of page charges. The article must therefore be hereby marked "*advertisement*" in accordance with 18 U.S.C. Section 1734 solely to indicate this fact.

were used for all studies. Mice were of matching age (mean: 99 days) and weight (mean: 30 g), and littermates were used whenever possible. All housing, surgical procedures, and experimental protocols were approved by the Institutional Animal Care and Use Committee.

Surgical procedures and blood pressure. Mice were anesthetized by intraperitoneal injection of ketamine (100 mg/ml)/xylazine (20 mg/ml) cocktail. Arterial blood pressure was measured using a catheter (Millar Instruments, Houston, TX) inserted into the right common carotid artery. The blood pressure was monitored for 15 min, and the average systolic, diastolic, and mean pressure were recorded. The ascending aorta, abdominal aorta, and left common carotid artery were exposed, and heparin (1,000 U/ml, ~50 U/mouse) was injected into the left ventricle to prevent blood clots during dissection. Small particles (30- to 90-μm diameter) of activated charcoal (Sigma, St. Louis, MO) were placed along the length of each artery on the ventral surface for measuring in vivo stretch and for calculating the longitudinal stretch ratio during mechanical testing. The carbon markers stick to the artery wall without adhesive, probably as a result of electrostatic effects. Images were recorded of each artery in vivo with a stereomicroscope coupled to a video camera. The arteries were removed, placed in a physiological saline solution (130 mM NaCl, 15 mM $NaHCO_3$, 5.5 mM dextrose, 4.7 mM KCl, 1.2 mM $MgSO_4 \cdot 7H_2O$, 1.2 mM KH_2PO_4, 0.026 mM EDTA, and 1.6 mM $CaCl_2$, pH 7.2), and images were recorded of each artery in the ex vivo state before compliance testing. Blood pressure and mechanical test data for all three arteries were not necessarily obtained for every mouse. The sample size for each data set is given in RESULTS.

Mechanical testing. The arteries were cannulated on specially designed stainless steel cannulas and mounted on a pressure and force arteriograph (Danish Myotechnology, Copenhagen, Denmark) (9, 10). The arteries were secured with silk surgical suture (size 10-0) tied at grooves machined into the end of each cannula. The experiments were performed in physiological saline solution at 37°C. The artery was transilluminated under an inverted microscope connected to a charge-coupled device camera and a computer. A central region along the artery length with identifiable carbon markers was chosen for diameter and length measurements. The arteriograph software continuously tracks the artery outer diameter by locating the change in pixel intensity between the illuminated artery and the dark background. The software was not designed to track the length markers, so the marker distance was determined manually from still images taken before each protocol. The distance between markers (l) was calculated using Image J software as described below. The arteriograph increases or decreases the intravascular (transmural) pressure of the artery segment by changing the fluid flow through the cannulas. The artery length was adjusted manually by turning a micrometer attached to one of the cannulas. The starting length for each artery was determined during three preconditioning cycles from 0 to 175 mmHg and was defined as the minimum length at which the artery did not significantly buckle in the longitudinal direction at 175 mmHg. At the starting length, the intravascular pressure was then increased from 0 to 175 mmHg for three cycles in steps of 25 mmHg (12 s/step). Preliminary data showed that the mechanical behavior of mouse arteries does not change with loading rate between continuous pressure increases of 7 mmHg/s (maximum for the system) and stepwise pressure increases of 60–300 s/25-mmHg step used in previous tests (9, 10). A value of 12 s/step was chosen to minimize experiment time while allowing operator supervision of the diameter tracking. After each protocol, the artery length was increased and the pressure was increased from 0 to 175 mmHg for three more cycles. The pressure, outer diameter, and longitudinal force were recorded at 1 Hz for each protocol. After mechanical testing, a narrow ring (1–2 mm long) was cut from the center of the artery and imaged to obtain the unloaded diameter and thickness. The artery boundaries were determined manually, and the dimensions were measured using Image J software.

In vivo lengths. Images were recorded of each artery in vivo with a stereomicroscope coupled to a video camera. After excision, the arteries were imaged in the ex vivo configuration floating in physiological saline solution. Image J software was used to determine the centroid of each carbon marker and calculate the length between successive markers. The in vivo longitudinal stretch ratio (λ_z^{iv}) was determined by dividing the in vivo distance (l_{iv}) by the ex vivo (unloaded) distance (L) for each pair of markers and was averaged for the length of the artery. Only markers visible in both in vivo and ex vivo images were measured. In some cases, the arteries looped or curved dramatically upon excision. In these cases, a line was drawn between successive markers following the curve of the artery, and the length of this line was used as the distance between markers.

Opening angle. Narrow rings (1–2 mm long) were cut along the length of the artery, and each ring was cut radially to measure the opening angle. In preliminary experiments, rings were cut from each artery after mechanical testing. However, it was difficult to remove arteries from the test setup without damage and to cut rings at the same longitudinal location in each artery. It also was difficult to cut rings from unpressurized arteries without collapsing the walls and changing the circular geometry. Consequently, opening angles were measured in arteries not used for mechanical testing. The mice were anesthetized and the arteries exposed as described above. Carbon particles were used to mark the ventral surface of the artery. Warm gelatin [14% in phosphate-buffered saline (PBS) at 37°C] mixed with dextran blue (4 mg/ml) for contrast was injected through the left ventricle into the ascending aorta and common carotid arteries. The descending aorta was tied off with a suture to force gelatin into the carotid arteries. For the abdominal aorta, gelatin was injected directly into the inferior end at the iliac bifurcation. Ice-cold PBS was then poured on top of the arteries to set the gelatin. The arteries were removed, and two or three rings were cut from the superior, central, and inferior portion of the abdominal and left common carotid arteries. Two or three rings were cut from the proximal ascending aorta. The gelatin prevented the artery walls from collapsing while rings were being cut and was removed from each ring before the radial cut was made. The rings were placed in room temperature PBS and cut radially at the ventral surface. After 30 min for equilibration, the opened ring was imaged and the opening angle was measured using custom-written scripts in Matlab software. The opening angle was defined as the angle subtended by the lines connecting the midpoint of the inner circumference with the ends of the ring (6, 11). Example opening angle measurements are shown in Fig. 7, *B* and *C*.

Data analysis. Pressure, outer diameter, longitudinal force, and marker length data from individual test protocols were converted to stress and stretch ratios. Although all three loading cycles were similar, the third cycle was used for further analysis. The deformed inner diameter and thickness were calculated by assuming constant wall volume (9):

$$d_i = \sqrt{d_o^2 - \frac{L(D_o^2 - D_i^2)}{l}} \qquad t = \frac{d_o - d_i}{2}, \quad T = \frac{D_o - D_i}{2} \qquad (1)$$

where d_i, d_o, l, and t are the deformed inner and outer diameters, length, and thickness and D_i, D_o, L, and T are the unloaded inner and outer diameters, length, and thickness.

Cylindrical coordinates are used in the stretch and stress notation with θ, z, and r referring to the circumferential, longitudinal, and radial axes, respectively. Shear was neglected because the markers along the length of the artery did not significantly rotate out of the image plane during loading cycles. The mean stretch ratios in each direction (λ_θ, λ_z, and λ_r) were calculated as (20)

$$\lambda_\theta = \frac{1}{2}\left[\frac{d_i}{D_i} + \frac{d_o}{D_o}\right] \qquad \lambda_z = \frac{l}{L} \qquad \lambda_r = \frac{t}{T}. \qquad (2)$$

In some cases, the longitudinal stretch ratio (λ_z^*) was calculated with respect to the in vivo length (l_{iv}):

$$\lambda_z^* = \frac{l}{l_{iv}} = \frac{\lambda_z}{\lambda_z^{iv}}. \qquad (3)$$

Table 1. *Pressure and geometry*

	Wild Type	ELN$^{+/-}$	*P*
Age, days	100 (4)	98 (4)	6.0E−2
Body weight, g	30 (3)	30 (4)	7.0E−1
Arterial pressure, mmHg			
Systolic	122 (28)	175 (19)	2.0E−5
Diastolic	80 (20)	107 (9)	5.0E−4
Mean	98 (23)	136 (10)	6.0E−5
Unloaded dimensions			
Outer diameter, μm			
Abdominal	568 (11)	469 (8)	2.0E−5
Ascending	1000 (12)	786 (12)	2.0E−5
Carotid	402 (10)	358 (7)	5.0E−3
Thickness, μm			
Abdominal	83 (4)	72 (4)	4.0E−2
Ascending	109 (6)	97 (7)	1.0E−2
Carotid	59 (4)	59 (4)	7.0E−1

Values are means (SD).

Assuming constant wall volume and a thin-walled tube, the mean stresses in the circumferential (σ_θ) and longitudinal (σ_z) directions were defined as

$$\sigma_\theta = \frac{P_i d_i}{d_o - d_i} \quad (4)$$

$$\sigma_z = \frac{4F + P_i \pi d_i^2}{\pi (d_o^2 - d_i^2)}, \quad (5)$$

where P_i is the inner pressure and F is the longitudinal force (21).

ANOVA or unpaired, two-tailed *t*-tests, assuming unequal variance, were used as appropriate to determine statistical differences between groups. $P < 0.05$ was considered significant.

RESULTS

Pressure and geometry. Consistent with previous results (10), we found that ELN$^{+/-}$ mice had 34–43% higher systolic, diastolic, and mean arterial pressure than wild-type mice. Despite comparable ages and body weights, the unloaded outer diameter of each artery was 11–21% smaller in ELN$^{+/-}$ mice than in wild-type mice. The unloaded thickness was smaller than wild-type in ELN$^{+/-}$ ascending aorta and abdominal artery and was not significantly different in left common carotid arteries (Table 1).

Mechanical testing. The mean outer diameter was smaller in ELN$^{+/-}$ than in wild-type arteries at each pressure, except for ascending aortas at 100 mmHg (Fig. 1, *A–C*). At the in vivo longitudinal stretch ratio (λ_z^{iv}), the mean force decreased slightly with increased pressure in abdominal and left common carotid arteries, with no significant differences between genotypes (Fig. 1, *D* and *F*). At λ_z^{iv}, the mean force decreased with increasing pressure in ascending aorta and was significantly lower in ELN$^{+/-}$ aortas for pressures between 75 and 125 mmHg (Fig. 1*E*). Figure 2 shows representative data from one artery in each group at different longitudinal stretch ratios (λ_z^*) calculated with respect to the in vivo length. The diameter at each pressure decreased and the force increased with increasing λ_z^*. For ascending aorta, the diameter-pressure relationship shifted downward by 1–3% for each successive 10% increase in λ_z^*. For abdominal and left common carotid arteries, the diameter-pressure relationship shifted downward by 1–3% for successive 10% increases in λ_z^* between 0.9 and 1.1. The relationship shifted more for steps farther from the in vivo length, with the downward shift increasing from 8 to 14% and

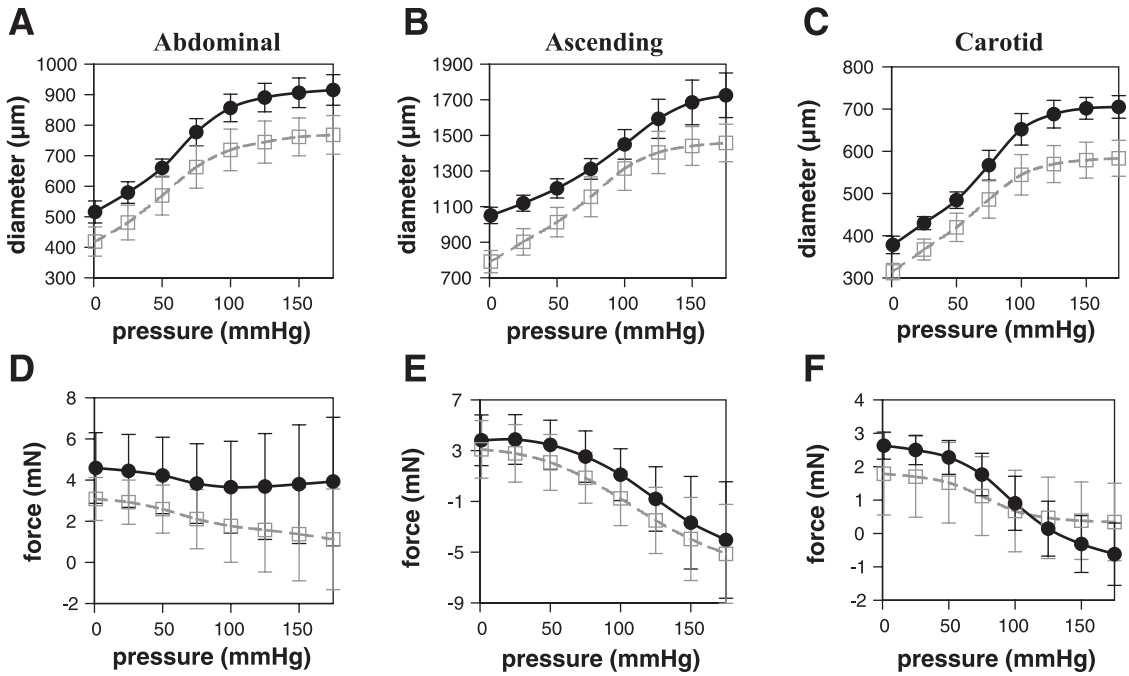

Fig. 1. Outer diameter and force vs. pressure for arteries from wild-type (●) and elastin-deficient (ELN$^{+/-}$; □) mice. Arteries were held at the in vivo longitudinal stretch ratio during testing ($\lambda_z^* = 1$). *A–C*: outer diameter vs. pressure for abdominal (*A*), ascending (*B*), and left common carotid arteries (*C*). There is a significant difference ($P < 0.05$) for all data points except ascending aorta at 100 mmHg ($P = 0.06$). *D–F*: longitudinal force vs. pressure is shown for abdominal (*D*), ascending (*E*), and left common carotid arteries (*F*). There is a significant difference for ascending aorta between 75 and 125 mmHg ($P = 0.03$, 0.01, and 0.04). Values are means (SD); $n = 6–10$ for each artery type.

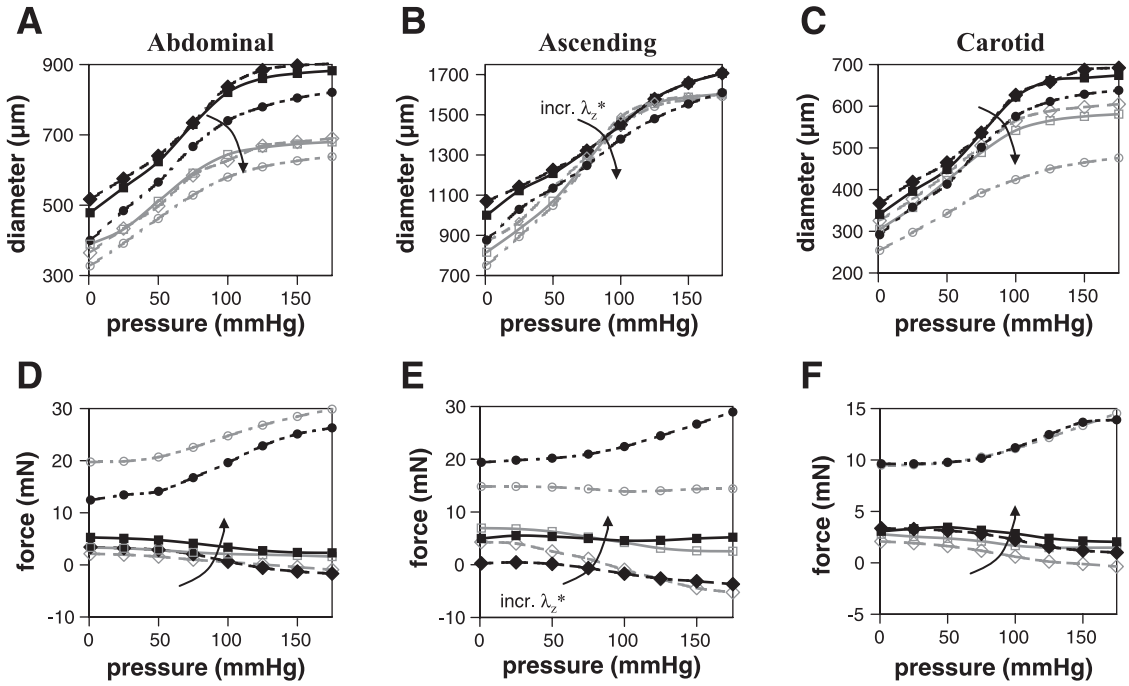

Fig. 2. Representative outer diameter and force vs. pressure for 1 artery in each group held at different longitudinal stretch ratios (λ_z^*) calculated with respect to the in vivo length. $\lambda_z^* = 0.9$, 1.0, and 1.2 (diamonds, squares, and circles, respectively) for abdominal aorta. $\lambda_z^* = 1.0$, 1.1, and 1.3 (diamonds, squares, and circles, respectively) for ascending and left common carotid arteries. The intermediate values of $\lambda_z^* = 1.1$ or 1.2 are omitted for clarity. *A–C*: outer diameter vs. pressure for abdominal (*A*), ascending (*B*), and left common carotid arteries (*C*). Curves shift downward with increasing λ_z^* (indicated by arrows, and labeled in *B*). *D–F*: longitudinal force vs. pressure for abdominal (*D*), ascending (*E*), and left common carotid arteries (*F*). Curves shift upward with increasing λ_z^* (indicated by arrows, and labeled in *E*). Wild type, filled symbols and solid lines; $ELN^{+/-}$, open symbols and shaded lines.

from 4 to 10% for successive 10% increases in λ_z^* between 1.2 and 1.5 for abdominal and left common carotid arteries, respectively. For most arteries, the longitudinal force decreased with pressure at $\lambda_z^* \leq 1.0$, remained constant around $\lambda_z^* = 1.1$, and increased with pressure at $\lambda_z^* > 1.1$. At $\lambda_z^* < 0.8$ for abdominal and $\lambda_z^* < 1.0$ for left common carotid arteries, the pressure could not be increased to 175 mmHg without the arteries bending longitudinally instead of stretching circumferentially. Bending during in vitro testing is caused by negative (compressive) longitudinal force at low longitudinal stretch and high pressure. Ascending aorta could not be tested at $\lambda_z^* <$ 0.9 because of the limited length of the arterial segment.

The circumferential stretch ratio and circumferential and longitudinal stresses at λ_z^{iv} ($\lambda_z^* = 1.0$) were averaged for each pressure step. Mean circumferential stretch ratios increased from 1.0 to 2.1, circumferential stresses increased from 0 to 370 kPa, and longitudinal stresses increased from 0 to 210 kPa for pressure increases from 0 to 175 mmHg for all arteries (Fig. 3). There are no significant differences between $ELN^{+/-}$ and wild-type abdominal aortas for the data shown in Fig. 3, *A*, *D*, or *G*. $ELN^{+/-}$ ascending aortas showed no significant difference from wild type for circumferential or longitudinal stresses (Fig. 3, *E* and *H*) but had significantly higher circumferential stretch ratios at pressures between 75 and 125 mmHg (Fig. 3*B*). $ELN^{+/-}$ left common carotid arteries showed no difference from wild type in circumferential stretch ratio or longitudinal stress (Fig. 3, *C* and *I*) but showed significantly lower circumferential stresses at all pressures >0 mmHg (Fig. 3*F*). At mean arterial pressure (wild type = 98 mmHg, $ELN^{+/-}$ = 136 mmHg), the longitudinal stress was similar for all arteries (Fig. 3, *G–I*) and the circumferential stretch ratio and stress were similar for abdominal and left common carotid arteries (Fig. 3, *A*, *C*, *D*, and *F*). At mean arterial pressure, the circumferential stretch ratio in $ELN^{+/-}$ ascending aorta was 20% higher and the circumferential stress was 68% higher than wild type (Fig. 3, *B* and *E*). The circumferential stress-stretch relationship at different λ_z^* was similar between genotypes for all arteries (representative data for 1 artery in each group in Fig. 4, *A–C*). The longitudinal stresses at equivalent circumferential stretch ratios were also similar (representative data for 1 artery in each group in Fig. 4, *D–F*). The abdominal aorta showed considerable variability in the longitudinal stress values at higher λ_z^* (Fig. 4*D*) due to the extreme nonlinearity of the longitudinal stress-stretch relationship (Fig. 5*A*).

For most arteries, the longitudinal stress-stretch relationship at zero pressure appeared similar between genotypes. The relationship was nonlinear and highly variable between individual arteries, with $ELN^{+/-}$ arteries showing more variation than wild type (Fig. 5). The data from individual arteries were not averaged because each artery was not stretched to identical longitudinal stretch values. Abdominal aortas showed the most nonlinear behavior, followed by left common carotid arteries and then ascending aortas. For abdominal aortas, wild-type arteries became nonlinear around $\lambda_z^* = 1.2$, whereas $ELN^{+/-}$ arteries became nonlinear around $\lambda_z^* = 1.1$ ($n = 4$) or $\lambda_z^* = 1.3$ ($n = 3$). Ascending aortas had a gradual nonlinear transition around $\lambda_z^* = 1.5$, although a few $ELN^{+/-}$ aortas had sharp nonlinear transitions not observed in the wild-type aortas. Left common carotid arteries became nonlinear at $\lambda_z^* = 1.5$–1.7. The trends were similar for nonzero pressures and when the longitudinal stretch ratio (λ_z) was calculated with respect to the unloaded length.

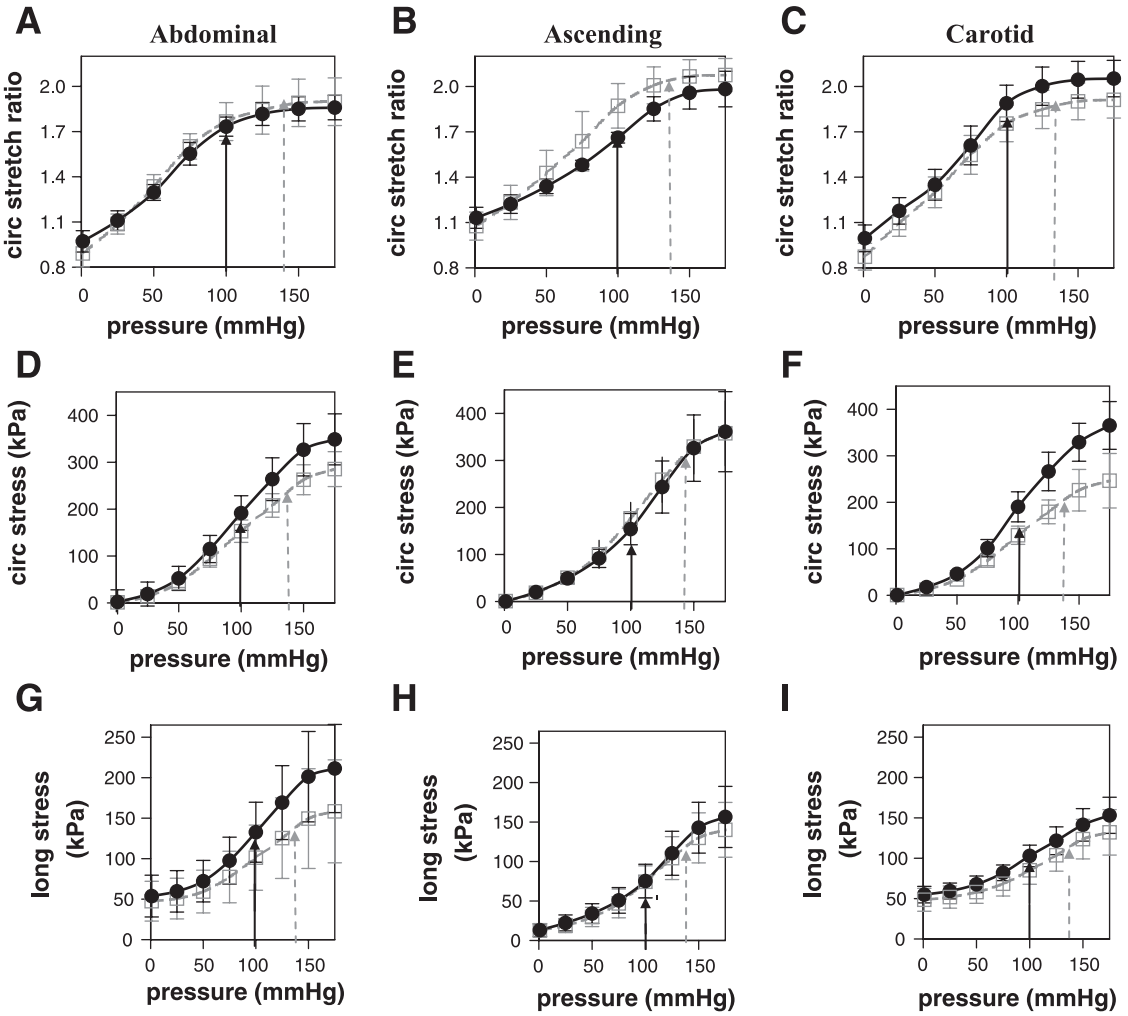

Fig. 3. Circumferential stretch ratio, circumferential stress, and longitudinal stress vs. pressure for wild-type (●) and ELN$^{+/-}$ (□) arteries held at the in vivo longitudinal stretch ratio ($\lambda_z^* = 1$). *A–C*: circumferential stretch ratio vs. pressure for abdominal (*A*), ascending (*B*), and left common carotid arteries (*C*). There is a significant difference for ascending aorta between 75 and 125 mmHg ($P = 0.04$, 0.003, and 0.01). *D–F*: circumferential stress vs. pressure for abdominal (*D*), ascending (*E*), and left common carotid arteries (*F*). There is a significant difference for left common carotid artery at pressures >0 mmHg ($P = 0.002–0.009$). *G–I*: longitudinal stress vs. pressure for abdominal (*G*), ascending (*H*), and left common carotid arteries (*I*). No significant difference is shown ($P > 0.05$) for any data. Values are means (SD); $n = 6–10$ for each artery type. Arrows (wild type, filled and solid; ELN$^{+/-}$, shaded and dashed) have been added at the mean arterial pressure for each genotype to show the physiological stretch ratios and stresses.

In vivo length. For abdominal and left common carotid arteries, λ_z^{iv} was smaller in ELN$^{+/-}$ than wild-type mice. For ascending aorta, λ_z^{iv} was not significantly different between ELN$^{+/-}$ and wild-type mice (Fig. 6*A*). For abdominal and left common carotid arteries, the ex vivo shape of the artery was different between ELN$^{+/-}$ and wild-type mice (Fig. 6, *B* and *D*). The ELN$^{+/-}$ arteries either looped (40% of left common carotids) or curved significantly (60% of left common carotids and 100% of abdominal aortas), whereas the wild-type arteries never looped and only curved slightly. The shape of the ascending aorta did not differ between ELN$^{+/-}$ and wild-type mice (Fig. 6*C*).

Opening angle. Compared with that of wild-type arteries, the mean opening angle of ELN$^{+/-}$ arteries was larger in ascending aorta and not significantly different in abdominal and left common carotid arteries (Fig. 7*A*). The opening angle for abdominal and left common carotid arteries did not vary significantly with longitudinal position in either genotype ($P = 0.3–0.8$). Representative opening angle measurements for wild-type and ELN$^{+/-}$ ascending aortas are shown in Fig. 7, *B* and *C*. The circumferential stretch ratio at the inner (d_i/D_i) and outer wall (d_o/D_o) of each artery type was calculated using the mean opening angle, unloaded dimensions, and dimensions at mean arterial pressure. In wild-type and ELN$^{+/-}$ mice, the circumferential stretch ratio was 10–13% higher at the inner wall for the abdominal aorta, 2–3% lower at the inner wall for the ascending aorta, and 15–17% higher at the inner wall for the left common carotid at mean arterial pressure. If the opening angle in ELN$^{+/-}$ ascending aorta were the same as that in wild type, the circumferential stretch ratio would be 1% higher at the inner wall than the outer wall. The higher opening angle in ELN$^{+/-}$ ascending aorta makes the transmural strain distribution more similar to that in wild type.

DISCUSSION

Characteristics of ELN$^{+/-}$ mice. ELN$^{+/-}$ mice exhibit many of the traits observed in human diseases associated with

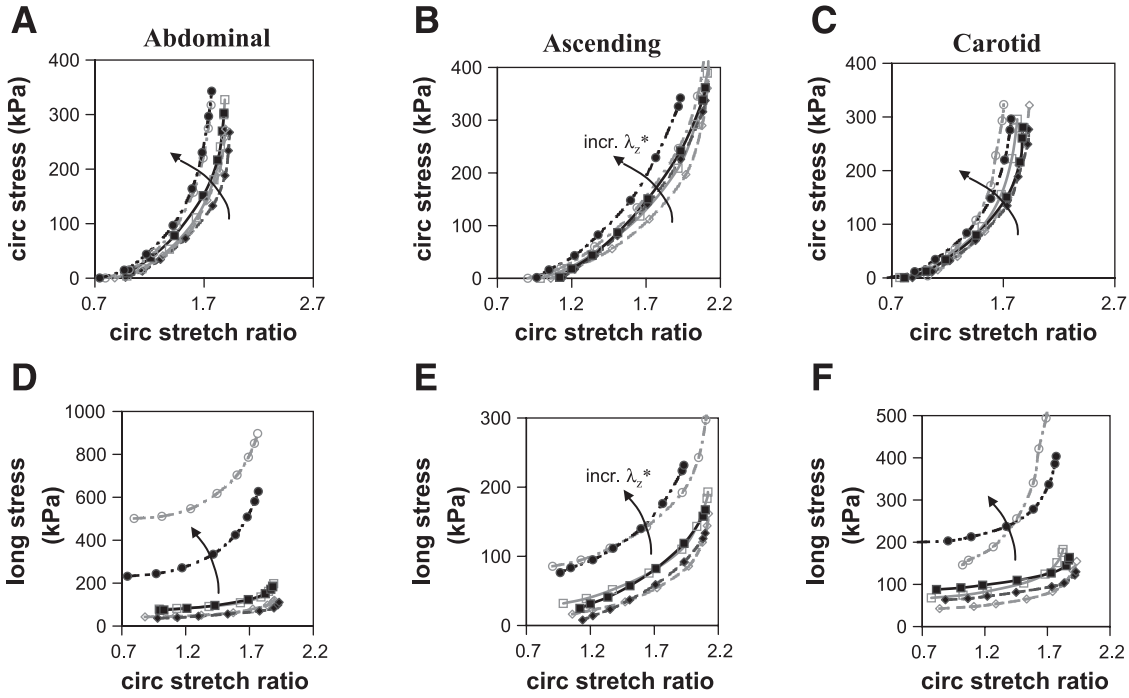

Fig. 4. Representative circumferential and longitudinal stress vs. circumferential stretch ratio for 1 artery in each group held at different longitudinal stretch ratios (λ_z^*) calculated with respect to the in vivo length. $\lambda_z^* = 0.9$, 1.0, and 1.2 (diamonds, squares, and circles, respectively) for abdominal aorta. $\lambda_z^* = 1.0$, 1.1, and 1.3 (diamonds, squares, and circles, respectively) for ascending and left common carotid arteries. The intermediate values of $\lambda_z^* = 1.1$ or 1.2 are omitted for clarity. *A–C*: circumferential stress vs. circumferential stretch ratio for abdominal (*A*), ascending (*B*), and left common carotid arteries (*C*). Curves shift leftward with increasing λ_z^* (indicated by arrows, and labeled in *B*). *D–F*: longitudinal stress vs. circumferential stretch ratio for abdominal (*D*), ascending (*E*), and left common carotid arteries (*F*). Curves shift upward with increasing λ_z^* (indicated by arrows, and labeled in *E*). Wild type, filled symbols and solid lines; $ELN^{+/-}$, open symbols and shaded lines.

elastin haploinsufficiency. Like SVAS patients, $ELN^{+/-}$ mice are hypertensive and have reduced arterial compliance and an increased number of lamellar units (10). $ELN^{+/-}$ arteries are useful for studying the effects of reduced elastin on arterial mechanics. However, we believe that the mechanical behavior of $ELN^{+/-}$ arteries is caused not only by reduced elastin but also by complex remodeling of the arterial wall in response to mechanical stimuli during development.

Effects of longitudinal stretch on arterial compliance. It is known that arterial compliance depends on longitudinal stretch and that arteries are in a stretched state in vivo (25). Despite these observations, the diameter-pressure relationship at the in vivo longitudinal stretch ratio (λ_z^{iv}) for both $ELN^{+/-}$ and wild-type arteries is similar to previous results obtained when longitudinal stretch was not considered (10, 19); $ELN^{+/-}$ arteries consistently have smaller diameters than wild-type arteries. We determined that the diameter-pressure relationship changes <3% within 10% of λ_z^{iv} and 2–8% (depending on the artery type) within 20% of λ_z^{iv}. Arteries cannot be inflated without buckling when held 10–20% below λ_z^{iv}. When stretched more than 20% above λ_z^{iv}, the high longitudinal forces cause arteries on glass cannulas, like those used in previous studies (10, 19), to slip off at the ends. The metal cannulas used in this study were designed with grooves at the end to hold the securing sutures and prevent artery slippage at high longitudinal stretch. As long as the artery is not buckling or slipping longitudinally during loading cycles, the diameter-pressure relationship will be close to that observed at λ_z^{iv}. If desired, λ_z^{iv} can be estimated by monitoring the slope of the force-pressure relationship. The longitudinal force-pressure relationship for both $ELN^{+/-}$ and wild-type arteries remains relatively constant or decreases slightly near λ_z^{iv}. This property has been

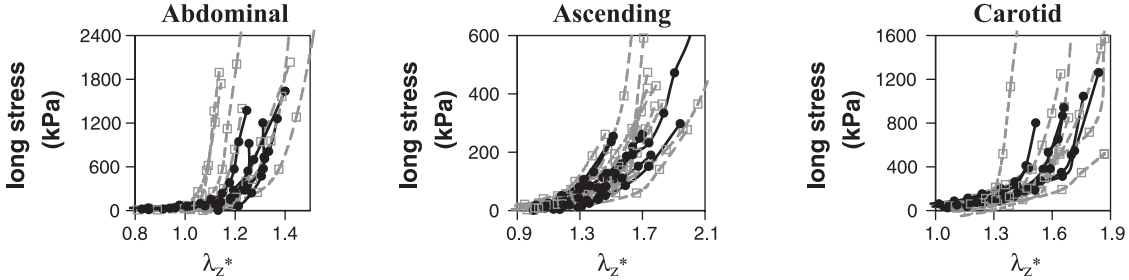

Fig. 5. Longitudinal stress at zero pressure vs. longitudinal stretch ratio (λ_z^*) calculated with respect to in vivo length for abdominal, ascending, and left common carotid arteries. Individual curves are shown for each specimen; $n = 6–10$ for each artery type. Relationships are similar for higher pressures and when the longitudinal stretch ratio (λ_z) is calculated with respect to the unloaded length. Wild type, filled symbols and solid lines; $ELN^{+/-}$, open symbols and shaded lines.

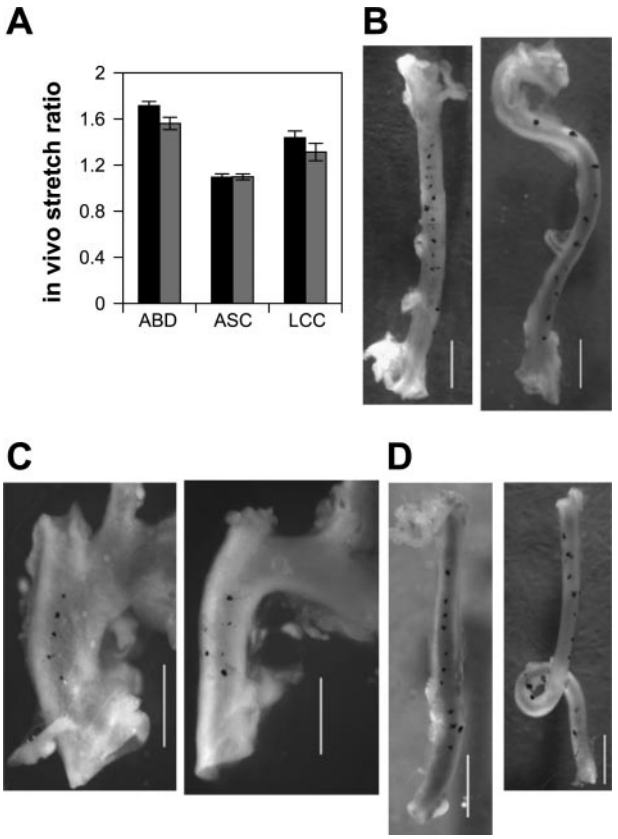

Fig. 6. In vivo longitudinal stretch in arterial segments. *A*: mean in vivo stretch ratio. Wild type, solid bars; $ELN^{+/-}$, shaded bars. Values are means (SD); n = 8–10 for each artery type. There is a significant difference for abdominal (P = 0.01) and left common carotid (P = 0.007) arteries but not for ascending aorta (P = 0.9). *B–D*: representative ex vivo images of abdominal (*B*), ascending (*C*), and left common carotid arteries (*D*): *left*, wild type; *right*, $ELN^{+/-}$. Scale bars, 1 mm.

previously documented in rat tail arteries (24), rat carotid arteries (25), and dog carotid arteries (7). Although measuring the longitudinal stretch ratio (λ_z) is not necessary for obtaining physiologically relevant outer diameter-pressure relationships, λ_z is necessary to calculate the deformed inner diameter (*Eq. 1*) and, consequently, the stretch ratios and stresses (*Eqs. 2*, *4*, and *5*). The inner diameter must be calculated, because tracking it throughout the loading cycle in large, relatively thick-walled arteries is often not possible.

Elastin production in vascular development. The smaller diameter in $ELN^{+/-}$ arteries may be the result of decreased elastin production during development. In mice, elastin production begins as pulsatile flow develops and peaks just after birth (17). Soon after birth, there are sharp increases in body weight, blood pressure, artery length, diameter, and thickness, and elastin and collagen content in mammalian arteries (3, 4, 13). In a newborn rat aorta, 65% of the medial volume is occupied by smooth muscle and 13% is occupied by elastin. At 4 wk of age, smooth muscle volume decreases to 40% and elastin volume increases to 48% (13). The elastin content in $ELN^{+/-}$ arteries is ~30% less than that in wild type when normalized to total protein, whereas the collagen content is unchanged (10). The cross-sectional area of most $ELN^{+/-}$ arteries is also ~30% less than that in wild type (calculated from Table 1). If the length of each $ELN^{+/-}$ artery is maintained and there is less elastin available to increase the artery cross-sectional area during growth, then the artery may develop with a smaller diameter. Hypertension in $ELN^{+/-}$ mice may be an adaptive mechanism to increase arterial diameter and consequently maintain cardiac output and perfusion pressure (10, 19).

Arterial remodeling. The diameter is smaller in $ELN^{+/-}$ arteries than in wild type, but the circumferential stretch ratio is the same or larger for the pressure range used in this study. For pressures between 75 and 125 mmHg, the circumferential stretch ratio is larger in $ELN^{+/-}$ ascending aorta than in wild type. This may be an adaptive mechanism, similar to hypertension, to increase the arterial diameter. Hypertension has limited potential for increasing the diameter because of arterial stiffening at high pressures (less change in diameter with the same increase in pressure). Increasing arterial diameter may be more important in the ascending aorta than other arteries to avoid left ventricular overload.

Increased pressure may increase arterial diameter, but it also increases the circumferential stress. In typical hypertension, the arterial geometry is subsequently remodeled (inner diameter decreases and thickness increases) to reduce the circumferential wall stress back to normal values (5). The diameter is decreased in $ELN^{+/-}$ arteries, but the thickness is not increased, and the thickness/lumen ratio (calculated from Table 1) is approximately the same in wild-type and $ELN^{+/-}$ arteries. Therefore, the remodeling response of $ELN^{+/-}$ arteries to hypertension is fundamentally different than that of wild-type arteries with induced hypertension. For both abdominal and left common carotid arteries, differences in mechanical behavior between wild-type and $ELN^{+/-}$ arteries lead to similar circumferential stresses at mean arterial pressure. In contrast, $ELN^{+/-}$ ascending aorta shows higher circumferential stress than wild type at mean arterial pressure.

Circumferential stress is related to the tension (T) in the arterial wall (T = pressure × inner radius). Tension in $ELN^{+/-}$ arteries is 42% higher than wild type in ascending aorta and 21% higher in abdominal and left common carotid arteries. If the tension is divided by the observed number of lamellae (estimated for ascending and abdominal aorta from Ref. 19 and measured from unpublished data in this study), then the tension/lamellae in $ELN^{+/-}$ arteries is 14% higher than that in

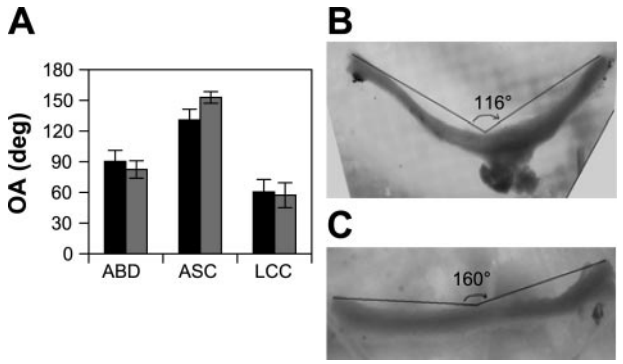

Fig. 7. Circumferential residual strain in arterial segments. *A*: mean opening angle (OA). Wild type, solid bars; $ELN^{+/-}$, shaded bars. Values are means (SD); n = 7 for each artery type. There is a significant difference for ascending aorta (P = 0.004) but not abdominal (P = 0.2) or left common carotid (P = 0.7) arteries. *B* and *C*: representative images of ascending aorta segments for wild type (*B*) and $ELN^{+/-}$ (*C*).

wild type in the ascending aorta and ~10% lower in the abdominal and left common carotid arteries. The tension/lamellae in all arteries for both genotypes is 0.9–1.3 Pa, which is within the range of 1–3 Pa found in most mammals (26). For the ascending aorta, differences in circumferential stress may be less important than maintaining diameter and tension/lamellae for arterial remodeling.

Relating mechanical properties to artery wall composition. Theoretically, the mechanical behavior of each artery can be related to the protein composition of the wall. It is believed that elastin behaves linearly and contributes to the circumferential and longitudinal stress-stretch relationship at low stretch, whereas collagen behaves nonlinearly and contributes at higher stretch (8). The wild-type aorta has the highest total elastin amount and elastin-to-collagen ratio (10), so it would be expected to have the most linear behavior and perhaps higher stresses at low stretch ratios. In the circumferential direction, the wild-type aorta shows the expected behavior; the stress-stretch relationship is more linear than the other arteries, with a higher slope at low stretch ratios and lower slope at high stretch ratios. In the longitudinal direction, both wild-type and $ELN^{+/-}$ ascending aortas show gradual increases in stress with increased stretch compared with the more nonlinear behavior (gradual increase in stress followed by a sharp increase past a certain stretch ratio) in abdominal and left common carotid arteries. The $ELN^{+/-}$ ascending aorta behaves like wild-type ascending aorta in the longitudinal direction, even though the elastin amount and elastin-to-collagen ratio are closer to values for wild-type abdominal and left common carotid arteries (10). One explanation for these data is that the ascending aorta has a greater proportion of elastin contributing mechanically in the longitudinal direction than the other arteries and that this property is maintained despite the reduced total elastin in the $ELN^{+/-}$ ascending aorta. The circumferential and longitudinal stress-stretch relationships at λ_z^{iv} for the wild-type arteries are qualitatively similar to the relationships measured by Guo and Kassab (14) in situ along the length of the aorta in C57BL/6 mice.

Differentiating between the circumferential and longitudinal stress-stretch relationships of the other artery types on the basis of wall composition is not possible. Because $ELN^{+/-}$ arteries have decreased elastin throughout development, adaptive remodeling may lessen the differences in mechanical behavior that would be expected if the elastin in a mature wild-type artery were suddenly reduced by 30%. The resulting small differences in mechanical behavior may be masked by measurement errors and interanimal variability. Other differences between $ELN^{+/-}$ and wild-type arteries, such as smaller diameter, more lamellae, and increased pressure, suggest that $ELN^{+/-}$ arteries are being remodeled in response to the mechanical stimuli during development. Several investigators have developed microstructural models to predict the mechanical behavior of arteries on the basis of relative amounts of elastin and collagen (2, 27). Our data show that changes in the relative amounts of elastin and collagen may not change the mechanical properties if the amounts of matrix proteins are altered from the start of development. Our data also show that changes in the mechanical properties may be different in the circumferential and longitudinal directions, possibly because of the arrangement and/or distribution of elastin and collagen in each artery type. These observations complicate any correlations between elastin and collagen amounts and mechanical behavior.

Elastin and residual strain. In vivo longitudinal stretch is lower in $ELN^{+/-}$ abdominal and left common carotid arteries, suggesting that reduced elastin does correlate with reduced longitudinal retraction (8). In vivo longitudinal stretch was similar between genotypes for ascending aorta, but the ascending aorta does not retract much upon excision and differences between genotypes may have been too small to measure in this study. Measuring the distance between arterial length markers was often complicated by the curvature of the artery, obscuring pieces of fat, and occasional shifting of the markers during artery handling. In addition to the differences in the in vivo longitudinal stretch, it was observed that $ELN^{+/-}$ arteries appeared "loose" in vivo and might be longer overall. The in vivo longitudinal stretch measured in wild-type arteries is consistent with other measurements in the same mouse strain (14, 15).

$ELN^{+/-}$ abdominal and left common carotid arteries loop or curve dramatically upon excision, whereas wild-type arteries never loop and only curve slightly. The change in shape upon excision may be caused by residual shear in the longitudinal-circumferential direction. Shear in this direction can be thought of as twist or torsion of the artery along its length, as if the ends were rotated in opposite directions. When markers were placed in a straight line down the artery length, they shifted into a diagonal line upon excision in both $ELN^{+/-}$ and wild-type abdominal aortas and left common carotid arteries. The shift was most obvious in $ELN^{+/-}$ left common carotid arteries, with the markers changing to the opposite side of the artery as it looped. Residual shear has been observed in the left ventricle of wild-type and tight-skin mice and was quantified by the out-of-plane warp angle in opening angle rings (23). We attempted to measure out-of-plane warp angle, but the specimens were too small for accurate measurements. Residual shear may be an adaptation to increased longitudinal stresses during development. Arterial geometry, retraction force, and pressure all contribute to longitudinal stress. Whereas arterial diameter and thickness can be reduced in response to mechanical stimuli, arterial length cannot be reduced in a similar manner (16). In hypertensive and/or older patients with reduced elastin, arteries often lengthen and may become tortuous (8). $ELN^{+/-}$ arteries may twist and possibly lengthen during growth in response to increased pressure and decreased retraction force caused by reduced elastin content. A combination of residual shear and decreased retraction force in the longitudinal direction will cause a cylindrical segment to form a loop when shortened.

The opening angle is larger in $ELN^{+/-}$ than in wild-type ascending aorta but not significantly different in abdominal and left common carotid arteries. Opening angle normalizes the circumferential strain through the artery wall (6), but sensitivity of the transmural strain distribution to opening angle is dependent on the arterial geometry. The geometry of the ascending aorta is more sensitive to changes in opening angle than the other arteries; therefore, increasing the opening angle in $ELN^{+/-}$ ascending aorta is an effective method to bring the transmural strain distribution near wild-type levels. The wild-type opening angles are consistent with other measurements in the same mouse strain (14, 15).

In conclusion, this study presents detailed mechanical test data comparing wild-type and $ELN^{+/-}$ mouse arteries. $ELN^{+/-}$ arteries have a smaller diameter than wild-type arteries at all pressures, but the circumferential stretch ratio is the same or greater. The circumferential mechanical behavior is relatively insensitive to longitudinal stretch near in vivo values; hence, in vivo stretch does not have to be explicitly measured to obtain physiologically relevant outer diameter-pressure relationships. $ELN^{+/-}$ abdominal and left common carotid arteries have an altered circumferential stress-pressure relationship that provides equivalent circumferential stresses at mean arterial pressure. $ELN^{+/-}$ ascending aortas have higher circumferential stresses at mean arterial pressure but similar tension/lamellae. $ELN^{+/-}$ abdominal and left common carotid arteries have lower in vivo longitudinal stretch, and $ELN^{+/-}$ ascending aortas have higher circumferential residual strains that normalize the transmural strain distribution at mean arterial pressure. The mechanical behavior of $ELN^{+/-}$ arteries is likely attributable to the decreased amount of elastin combined with adaptive remodeling during vascular development. This remodeling process is an important consideration for human diseases, such as SVAS, in which alterations in matrix proteins are present at birth.

ACKNOWLEDGMENTS

Chris Ciliberto is gratefully acknowledged for mouse care and genotyping.

GRANTS

This study was funded by National Institutes of Health Training Grant HL-007916 (to J. E. Wagenseil) and National Heart, Lung, and Blood Institute Grants HL-53325, HL-62295, and HL-074138 (to R. P. Mecham).

REFERENCES

1. **Arteaga-Solis E, Gayraud B, and Ramirez F.** Elastic and collagenous networks in vascular diseases. *Cell Struct Funct* 25: 69–72, 2000.
2. **Bank AJ, Wang H, Holte JE, Mullen K, Shammas R, and Kubo SH.** Contribution of collagen, elastin, and smooth muscle to in vivo human brachial artery wall stress and elastic modulus. *Circulation* 94: 3263–3270, 1996.
3. **Bendeck MP, Keeley FW, and Langille BL.** Perinatal accumulation of arterial wall constituents: relation to hemodynamic changes at birth. *Am J Physiol Heart Circ Physiol* 267: H2268–H2279, 1994.
4. **Berry CL, Looker T, and Germain J.** The growth and development of the rat aorta. I. Morphological aspects. *J Anat* 113: 1–16, 1972.
5. **Briones AM, Gonzalez JM, Somoza B, Giraldo J, Daly CJ, Vila E, Gonzalez MC, McGrath JC, and Arribas SM.** Role of elastin in spontaneously hypertensive rat small mesenteric artery remodelling. *J Physiol* 552: 185–195, 2003.
6. **Chuong CJ and Fung YC.** On residual stresses in arteries. *J Biomech Eng* 108: 189–192, 1986.
7. **Dobrin PB.** Biaxial anisotropy of dog carotid artery: estimation of circumferential elastic modulus. *J Biomech* 19: 351–358, 1986.
8. **Dobrin PB.** Physiology and pathophysiology of blood vessels. In: *The Basic Science of Vascular Disease*, edited by Sidawy AN, Sumpio BE, and DePalma RG. New York: Futura, 1997, p. 69–105.
9. **Faury G, Maher GM, Li DY, Keating MT, Mecham RP, and Boyle WA.** Relation between outer and luminal diameter in cannulated arteries. *Am J Physiol Heart Circ Physiol* 277: H1745–H1753, 1999.
10. **Faury G, Pezet M, Knutsen RH, Boyle WA, Heximer SP, McLean SE, Minkes RK, Blumer KJ, Kovacs A, Kelly DP, Li DY, Starcher B, and Mecham RP.** Developmental adaptation of the mouse cardiovascular system to elastin haploinsufficiency. *J Clin Invest* 112: 1419–1428, 2003.
11. **Fung YC.** *Biomechanics: Mechanical Properties of Living Tissues*. New York: Springer, 1993.
12. **Fung YC and Liu SQ.** Strain distribution in small blood vessels with zero-stress state taken into consideration. *Am J Physiol Heart Circ Physiol* 262: H544–H552, 1992.
13. **Gerrity RG and Cliff WJ.** The aortic tunica media of the developing rat. I. Quantitative stereologic and biochemical analysis. *Lab Invest* 32: 585–600, 1975.
14. **Guo X and Kassab GS.** Variation of mechanical properties along the length of the aorta in C57bl/6 mice. *Am J Physiol Heart Circ Physiol* 285: H2614–H2622, 2003.
15. **Guo X, Kono Y, Mattrey R, and Kassab GS.** Morphometry and strain distribution of the C57BL/6 mouse aorta. *Am J Physiol Heart Circ Physiol* 283: H1829–H1837, 2002.
16. **Jackson ZS, Gotlieb AI, and Langille BL.** Wall tissue remodeling regulates longitudinal tension in arteries. *Circ Res* 90: 918–925, 2002.
17. **Kelleher CM, McLean SE, and Mecham RP.** Vascular extracellular matrix and aortic development. *Curr Top Dev Biol* 62: 153–188, 2004.
18. **Li DY, Brooke B, Davis EC, Mecham RP, Sorensen LK, Boak BB, Eichwald E, and Keating MT.** Elastin is an essential determinant of arterial morphogenesis. *Nature* 393: 276–280, 1998.
19. **Li DY, Faury G, Taylor DG, Davis EC, Boyle WA, Mecham RP, Stenzel P, Boak B, and Keating MT.** Novel arterial pathology in mice and humans hemizygous for elastin. *J Clin Invest* 102: 1783–1787, 1998.
20. **Malvern LE.** *Introduction to the Mechanics of a Continuous Medium*. Englewood Cliffs, NJ: Prentice-Hall, 1969.
21. **Matsumoto T and Hayashi K.** Stress and strain distribution in hypertensive and normotensive rat aorta considering residual strain. *J Biomech Eng* 118: 62–73, 1996.
22. **Mecham RP.** Overview of extracellular matrix. In: *Current Protocols in Cell Biology*. New York: Wiley, 1998, p. 10.11.11–10.11.14.
23. **Omens JH, Rockman HA, and Covell JW.** Passive ventricular mechanics in tight-skin mice. *Am J Physiol Heart Circ Physiol* 266: H1169–H1176, 1994.
24. **Pascale K.** Bidimensional passive and active mechanical behavior of rat tail artery segments in vitro. *Basic Res Cardiol* 84: 442–448, 1989.
25. **Weizsacker HW, Lambert H, and Pascale K.** Analysis of the passive mechanical properties of rat carotid arteries. *J Biomech* 16: 703–715, 1983.
26. **Wolinsky H and Glagov S.** A lamellar unit of aortic medial structure and function in mammals. *Circ Res* 20: 99–111, 1967.
27. **Zulliger MA, Fridez P, Hayashi K, and Stergiopulos N.** A strain energy function for arteries accounting for wall composition and structure. *J Biomech* 37: 989–1000, 2004.